frontiers in Energy Research

ORIGINAL RESEARCH
published: 28 March 2022
doi: 10.3389/fenrg.2022.878088

Effect of Dimethyl Formamide (DMF) on Vanadium Reloading Over V-Ti SCR Catalyst

Hao Song, Jiangmin Guo, Shaojun Liu, Yu Zhang, Weihong Wu, Chenghang Zheng and Xiang Gao**

State Key Lab of Clean Energy Utilization, State Environmental Protection Center for Coal-Fired Air Pollution Control, Zhejiang University, Hangzhou, China

Active components reloading is critical process for the catalyst regeneration, which is limited by the low adsorption capacity and unwilling distribution of desired components to the catalyst surface. Herein we demonstrated that with dimethyl formamide(DMF) modification and sequentially reloading of vanadium, the traditional V-Ti SCR catalyst, which uses vanadium as the active components and titanium as the carrier, showed the significantly improved DeNOx performance, owing to the increased adsorption capacity and desired distribution of vanadium. When the DMF concentration was 6%, the adsorption capacity of the promoted catalyst was 3.58 and 6.57 mg/g under vanadyl ion concentrations of 1.5 and 3 g/L, respectively, 135 and 147% higher than that of the original catalyst. Adsorption kinetics demonstrated that the pseudo-second-order kinetic model better describes the process by which vanadyl ions adsorb onto the catalyst. In addition, the adsorption equilibrium indicated that Langmuir model was a closer fit for the vanadyl ion adsorption to the promoted catalyst. After DMF modification, the vanadyl ions were first adsorbed onto the functional groups on the catalyst surface, substantially increasing the vanadium loading on the catalyst surface while limiting the increase in vanadium content within the interior of catalyst, which was conducive to enhancing the DeNOx activity and reducing the increase in the SO_2/SO_3 conversion. When the vanadium adsorption capacity was 3.5 mg/g, the increase in the DeNOx activity of the promoted catalyst was 68.1% higher than that of the original catalyst, whereas the increase in SO_2/SO_3 conversion was 28.9% lower than that of the original catalyst. Thus, in the regeneration of SCR catalysts vanadium initial concentration and loading could be reduced.

Keywords: SCR, V-Ti catalyst, vanadium reloading, DMF, adsorption

OPEN ACCESS

Edited by:
Xuesen Du,
Chongqing University, China

Reviewed by:
Shan Ren,
Chongqing University, China
Zhao-Bin Ding,
Sun Yat-sen University, China

****Correspondence:***
Shaojun Liu
phoenix205@zju.edu.cn
Xiang Gao
xgao1@zju.edu.cn

Specialty section:
This article was submitted to Advanced Clean Fuel Technologies, a section of the journal Frontiers in Energy Research

Received: *17 February 2022*
Accepted: *14 March 2022*
Published: *28 March 2022*

Citation:
Song H, Guo J, Liu S, Zhang Y, Wu W, Zheng C and Gao X (2022) Effect of Dimethyl Formamide (DMF) on Vanadium Reloading Over V-Ti SCR Catalyst. Front. Energy Res. 10:878088. doi: 10.3389/fenrg.2022.878088

INTRODUCTION

The catalyst is the core of selective catalytic reduction (SCR) flue gas denitrification (DeNOx) technology, and catalyst performance directly determines the stability of DeNOx efficiency in SCR DeNOx systems. The optimal operating temperature of SCR catalysis is 300–400°C (Busca et al., 1998; Forzatti, 2001). In the DeNOx process, the catalyst is typically placed between the economizer and air preheater. The high ash content at this position causes problems such as 1) catalyst poisoning caused by various elements (alkali metals, alkaline Earth metals, and heavy

metals) contained in coal (Kong et al., 2015a; Kong et al., 2015b; Kong et al., 2019; Yao et al., 2020; Zhang et al., 2020); 2) catalyst clogging and attrition ascribable to the deposition of fly ash, including large particles (Tanno et al., 2010); 3) catalyst sintering attributable to prolonged high-temperature operations (Xi et al., 2020); 4) volatilization of active components caused by chlorine ions in flue gas (Xiong et al., 2020); and 5) mechanical wear. These problems explain the relatively short lifespan of SCR catalysts in industrial applications (3–4 years). The lifespan of such catalysts can be extended through regeneration, which is also an effective method for handling deactivated SCR catalysts.

Numerous studies on the washing and regeneration of deactivated catalysts have been conducted (Khodayari and Ingemar Odenbrand, 2001; Khodayari and Odenbrand, 2001; Yu et al., 2013; Peng et al., 2015; Li et al., 2016). The active component, vanadium oxide (V_2O_5), may be lost during the washing process, and SCR catalysts also lose some V_2O_5 during their operation. Therefore, SCR catalysts must be supplemented with active components after washing. Furthermore, for the purpose of simultaneous Mercury oxidation or full load DeNOx improvement, active components must be reloaded into the catalysts (Song et al., 2018a; Song et al., 2018b). Because SCR catalysts are all monolithic catalysts, reloading the active components through incipient wetness impregnation is challenging. Instead, the active components must be loaded through excessive impregnation. In this context, the core problem concerns how to improve the adsorption of metal ions by SCR catalysts in the solution. Moreover, SCR reactions are associated with the wall thickness of catalysts; studies have reported that SCR reactions occur only within 0.1 mm thin layer of the catalyst wall due to the high reaction rate, whereas side reactions, such as sulfur dioxide (SO_2) oxidation occur within the entire catalyst wall (Tronconi et al., 1994; Orsenigo et al., 1996; Dunn et al., 1998; Tronconi et al., 1999; Forzatti et al., 2000; Jiang et al., 2019). Therefore, precisely controlling the loading of active components may be beneficial to the SCR process.

Research on wastewater treatment reveals that mineral materials have excellent adsorption capacity for metal ions. Moreover, the exposure of numerous active groups (e.g., hydroxyl groups) on mineral surfaces enables bonding with ions. Various researchers have modified mineral particles to increase the surface functional groups such that the adsorption capacity of metal ions by mineral materials can be enhanced. In one study, a silane coupling agent was allowed to react with and bond to active groups on the surface of mineral powder (Yuan et al., 2013) The general chemical formula of the silane coupling agent is $(OR)_3Si\text{-}R_2\text{-}R_1$, where R_1 is used to increase the adsorption capacity of pollutants and R_2 is used to promote contact between pollutants and adsorption sites through structural modifications. For example, Addy (Addy et al., 2012) bonded a silane coupling agent with a chelating functional group on the surface of montmorillonite, notably improving the adsorption capacity of montmorillonite to heavy metal cations under acidic conditions. Luo (Luo et al., 2014) modified hydrocarbyl groups on the surface of perlite into amino functional groups, substantially enhancing the adsorption capacity of humic acid.

The carrier of SCR catalysts is titanium dioxide, which is rich in hydroxyl groups on the surface. Therefore, in this study, dimethyl formamide (DMF) was introduced to the surface of the SCR catalyst, improving its adsorption of active components as well as DeNOx activity.

MATERIALS AND METHODS

The SCR catalyst used herein was provided by Zhejiang Zheneng Catalyst Co., Ltd. The catalysts had a honeycomb structure with an inner wall thickness of 0.7 mm, a pore diameter of 6.1 mm, and 22 × 22 catalyst pores. The catalyst was cut into unit blocks of 50 mm × 50 mm × 200 mm for experimental use.

To prepare an organic solution, a certain volume of DMF was accurately weighed and placed into deionized water to configure different concentrations of solutions(2, 4, 6, 8, 10%), after which it was stirred continuously for 6 h at 60°C. Subsequently, the SCR catalyst unit block was ultrasonically cleaned for 20 min, dried at 120°C for 2 h, and then immersed into the organic solution under ultrasonication at 60°C for 2 h. Subsequently, the catalyst was dried at 80°C for 12 h, becoming a promoted (DMF modified) SCR catalyst.

Certain amounts of ammonium metavanadate and oxalic acid were accurately weighed and placed into deionized water to configure different concentrations of solutions(1.5 g/L, 3 g/L), stirred thoroughly over 2 h at 60°C. This solution was set aside for later use. The molar ratio of ammonium metavanadate and oxalic acid was 1:2. The mixed aqueous solution reacted at 60°C, and the color changed from yellow (VO_2^+) to green and finally to dark blue (VO^{2+}). Subsequently, the original and promoted SCR catalysts were placed into the ammonium metavanadate solution at a certain concentration to absorb vanadyl ions at a certain temperature and time. Afterward, the catalysts were dried at 120°C for 6 h before being calcined in a muffle furnace for 5 h at 400°C. This process yielded reloaded SCR catalysts.

Using a test bench for evaluating the performance of monolithic catalysts, the DeNOx activity and SO_2/SO_3 conversion of the catalysts were examined.

For the DeNOx activity, the formula is as follows:

$$k = -\frac{V_f}{S_c} \times In\left(1 - \frac{\eta}{100}\right) \quad (1)$$

Where k is the DeNOx activity, m/h; V_f is the flow rate through the monolithic catalyst, m^3/h; Sc is the superficial area of the monolithic sample, m^2; η is the efficient of DeNOx, %.

To analyze the adsorption of vanadyl ions by the SCR catalysts, the concentration of vanadyl ions in the vanadium solution was determined before and after adsorption through inductively coupled plasma optical emission spectrometry. The formula for calculating the adsorption capacity of the SCR catalysts is as follows:

$$q_e = (C_0 - C_e)\frac{V}{m} \quad (2)$$

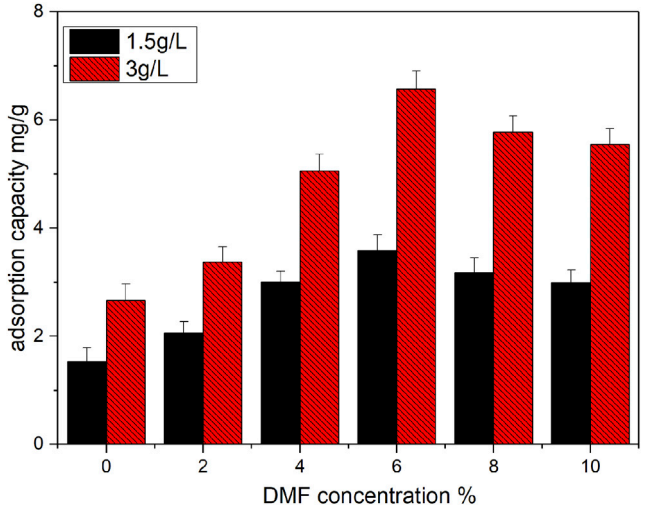

FIGURE 1 | Effect of DMF concentration on adsorption of vanadium ion (vanadium ion concentration: 1.5 g/L and 3 g/L, adsorption temperature: 50°C, adsorption time: 2 h).

where q_e is the equilibrium loading of the SCR catalysts (mg/g); C_0 and C_e are the initial and equilibrium concentrations of vanadyl ions in the solution (mg/L), respectively; V is the volume of the vanadyl ion solution (L); and m is the mass of the SCR catalysts (g).

RESULTS AND DISCUSSION

Effect of DMF Concentration

As shown in **Figure 1**, without DMF modification, the adsorption capacity of the original catalyst for vanadyl ions was relatively low, at 1.52 and 2.66 mg/g for vanadyl ion concentrations of 1.5 and 3 g/L, respectively. This indicates that vanadyl ion adsorption before catalyst modification was primarily dependent on weak chemical adsorption and physical adsorption. With the increase in the concentration of the organic solution, the adsorption capacity of the promoted SCR catalyst on vanadyl ions increased gradually, peaking when the DMF concentration was 6%. The adsorption capacities of the promoted catalysts at vanadyl ion concentrations of 1.5 and 3 g/L were 3.58 and 6.57 mg/g, respectively, 135 and 147% higher than those of the original catalyst, and the adsorption capacity of the promoted catalysts was substantially improved. However, when the organic solution concentration exceeded 6%, the adsorption capacity of the promoted catalyst decreased with increasing concentration. This indicated that there are optimum conditions for DMF modification, which are closely related to the modification process. As the concentration of organic compounds in the solution increased gradually, the number of organic functional groups anchored to the catalyst surface also increased gradually, thereby increasing the number of adsorption sites on the catalyst surface. However, when the number of anchored groups passed the optimum value, the interaction between groups may occurs, perhaps hindering the capture of vanadium ions.

Effect of Adsorption Time

According to **Figure 2**, under three different initial vanadyl ion concentrations, the adsorption capacity of vanadyl ions on the original and promoted catalysts increased rapidly and then slowed gradually, reaching an adsorption equilibrium. The rate by which vanadyl ions were adsorbed onto the catalyst accelerated, and the higher the initial concentration of vanadyl ions was, the steeper the initial adsorption curve and the greater the adsorption capacity became. Regarding the original catalyst, the higher the initial concentration of vanadyl ions was, the less time it took for the adsorption equilibrium to be reached. When the vanadyl ion concentrations were 0.5 and 2.5 g/L, 60–90 min elapsed before the adsorption capacity exceeded 90%. When the vanadyl ion concentration was 5 g/L, the adsorption capacity exceeded 90% in 30 min. The above phenomena could be explained as follows: when the vanadyl ion concentration was high, the diffusion rate was faster; therefore, the adsorption equilibrium was reached in a shorter time.

Effect of Adsorption Temperature

Figure 3 displays the effect of adsorption temperature on the adsorption of vanadyl ions onto the catalysts. The adsorption temperatures were 20, 35 and 50°C. At all concentrations and temperatures, the equilibrium adsorption capacity of the promoted catalyst for vanadyl ions was considerably higher than that of the original catalyst. This indicated that the promoted catalyst increased the number of functional groups on the catalyst surface and stimulated the adsorption of vanadyl ions on the catalyst, thereby facilitating the reloading of active components during catalyst regeneration. The adsorption capacity of the catalyst to vanadyl ions increased as the initial vanadyl ion concentration increased, but the rate of increase began to slow when the concentration of vanadyl ions was 3–5 g/L. Moreover, the adsorption capacity of both catalysts increased with the temperature. When the vanadyl ion concentration was 2.5 g/L, as the temperature increased from 20 to 50°C, the adsorption capacity of vanadyl ions on the original catalyst increased from 1.81 to 2.47 mg/g (a 36.5% increase), whereas the adsorption capacity of the promoted catalyst for vanadyl ions increased from 3.31 to 5.75 mg/g (a 73.7% increase). This result demonstrated that temperature had a stronger effect on the adsorption of the promoted catalyst than on that of the original catalyst. A plausible explanation is that the adsorption of vanadyl ions onto a catalyst is an endothermic process, and with the increase in temperature, the migration rate of vanadyl ions in water increases, thereby improving the adsorption of vanadyl ions by the catalyst (Wang et al., 2013).

Adsorption Kinetics

A kinetic model of adsorption was fitted to the experimental adsorption data. For analysis, the reaction-based pseudo-first-

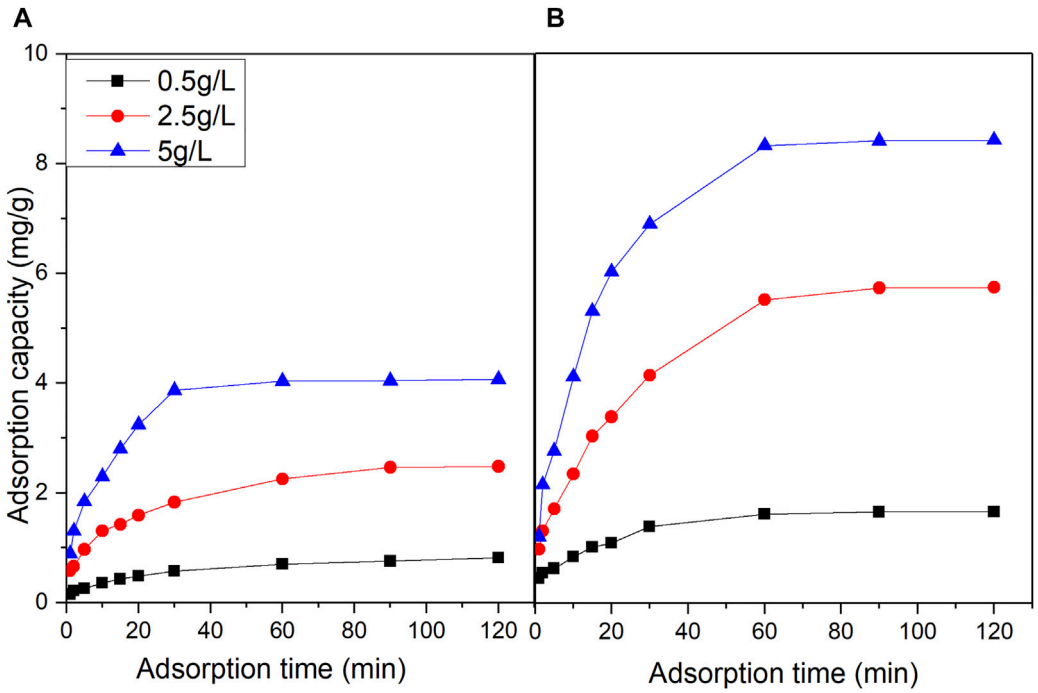

FIGURE 2 | Effect of time on vanadium ion adsorption **(A)** original catalyst **(B)** promoted catalyst(vanadium ion concentration: 0.5, 2.5, 5 g/L adsorption temperature: 50°C, DMF concentration: 6%).

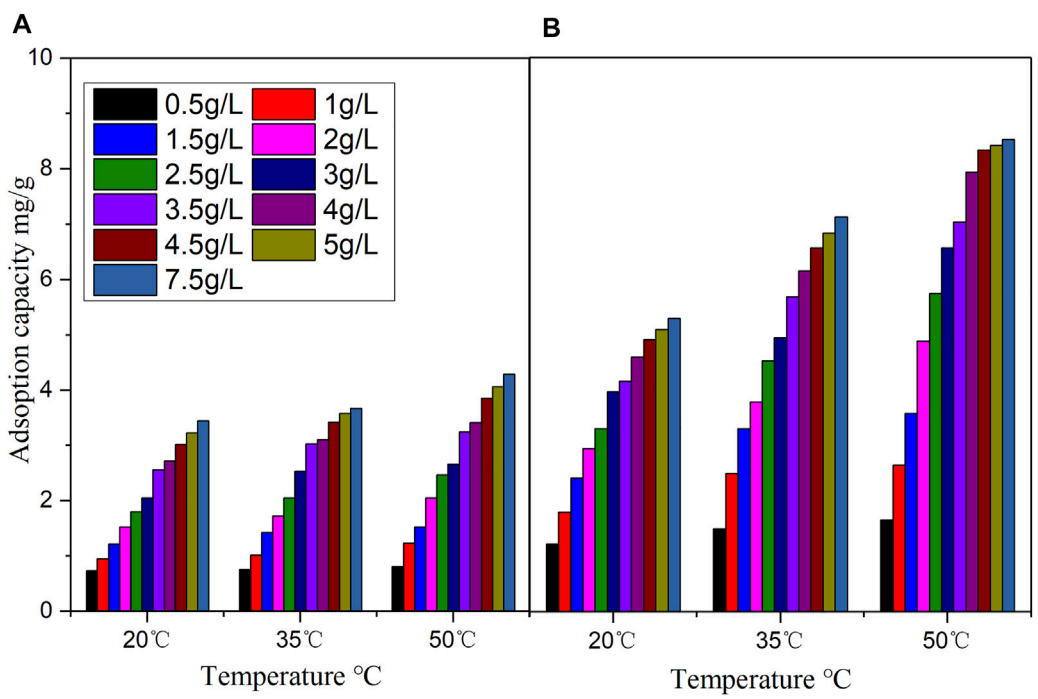

FIGURE 3 | Effect of temperature on vanadium ion adsorption **(A)** original catalyst **(B)** promoted catalyst (adsorption time: 2 h, DMF concentration: 6%).

TABLE 1 | Kinetics parameters for the adsorption of vanadium ion onto original catalyst.

Kinetics model	Parameters	Vanadium ion concentration		
		0.5 g/L	2.5 g/L	5 g/L
	$q_{e,exp}$(mg/g)	0.81	2.48	4.06
Pseudo-first-order	k_1(/min)	0.0267	0.0464	0.0595
	$q_{e,cal}$(mg/g)	0.605	2.139	2.67
	R^2	0.9877	0.9589	0.9213
Pseudo-second-order	k_2(g/(g·min)	0.0974	0.0393	0.0399
	$q_{e,cal}$(mg/g)	0.865	2.661	4.299
	R^2	0.9887	0.9926	0.9966

TABLE 2 | Kinetics parameters for the adsorption of vanadium ion onto promoted catalyst.

Kinetics model	Parameters	Vanadium ion concentration		
		0.5 g/L	2.5 g/L	5 g/L
	$q_{e,exp}$(mg/g)	1.66	5.75	8.42
Pseudo-first-order	k_1(/min)	0.0613	0.0643	0.0728
	$q_{e,cal}$(mg/g)	1.499	6.658	8.853
	R^2	0.9917	0.9634	0.9916
Pseudo-second-order	k_2(g/(g·min)	0.0686	0.0121	0.0116
	$q_{e,cal}$(mg/g)	1.786	6.41	9.192
	R^2	0.9937	0.9878	0.9966

order and pseudo-second-order kinetic models (Ren et al., 2020) and the Weber–Morris intraparticle diffusion model were employed for analysis.

The pseudo-first-order kinetic model is expressed as follows:

$$\frac{dq_t}{dt} = k_1 (q_e - q_t) \tag{3}$$

where q_e is the equilibrium adsorption capacity of the adsorbent (mg/g); q_t is the adsorption capacity at the adsorption time t (mg/g); and k_1 is the adsorption rate constant of the pseudo-first-order kinetic equation (mg/gmin).

The pseudo-second-order kinetic model equation can be expressed as follows:

$$\frac{dq_t}{dt} = k_2 (q_e - q_t)^2 \tag{4}$$

where k_2 is the equilibrium rate constant of the pseudo-second-order kinetic equation (mg/gmin).

The calculated values of the kinetic parameters and the corresponding coefficient of determination (R^2) are shown in **Tables 1**, **2**. **Figures 4**, **5** present the fitting results of the pseudo-first-order and pseudo-second-order kinetic models achieved under various types of catalysts and various initial vanadyl ion concentrations. The data were better fitted to the pseudo-second-order kinetic model, indicating that the adsorption rate was proportional to the square of the unconsumed adsorption sites (Gao et al., 2014).

In general, adsorption kinetics can be controlled by one or more steps, including: 1) bulk diffusion, the migration of vanadyl ions from the bulk solution to the boundary layer around the catalyst; 2) interparticle diffusion, the diffusion of vanadyl ions from the boundary layer to the external catalyst surface; 3) intraparticle diffusion, the diffusion of vanadyl ions to internal sites of the catalyst; and 4) surface adsorption, the adsorption of vanadyl ions to external and internal surfaces of the catalyst through physical and chemical adsorption or surface complexation. In general, surface adsorption may have faster reaction rate while interparticle or intraparticle diffusion exhibit lower rates. To verify this speculation, the adsorption process of vanadyl ions was fitted and analyzed using the Weber–Morris intraparticle diffusion model, which can be presented as follows:

$$q_t = k_i t^{0.5} + C \tag{5}$$

where k_i is the intraparticle diffusion rate constant (mg/gmin$^{0.5}$) and C is the adsorption constant. When the

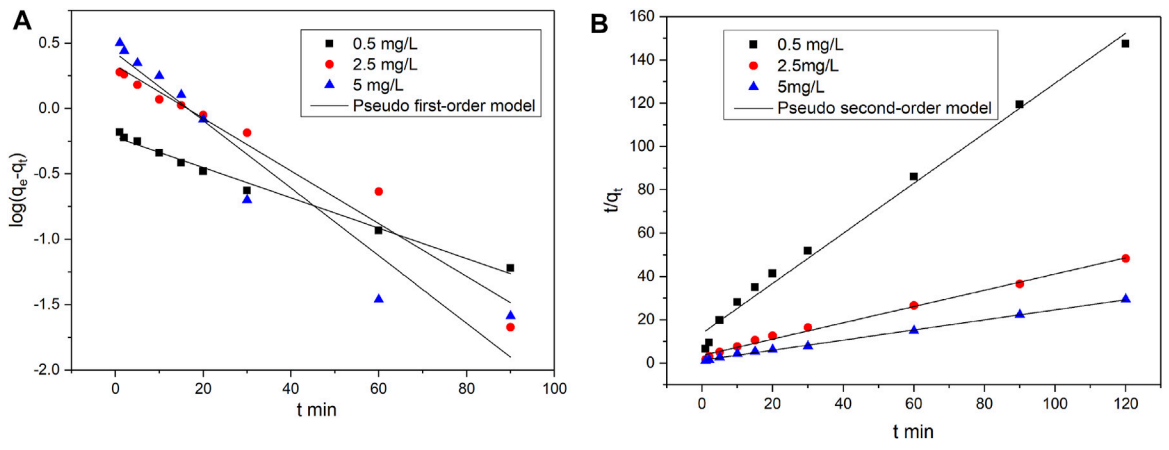

FIGURE 4 | Nonlinear fits of pseudo-first order and pseudo-second order kinetics models for vanadium ion adsorption by original catalyst. **(A)** Pseudo first-order model fitting; **(B)** Pseudo second-order model fitting.

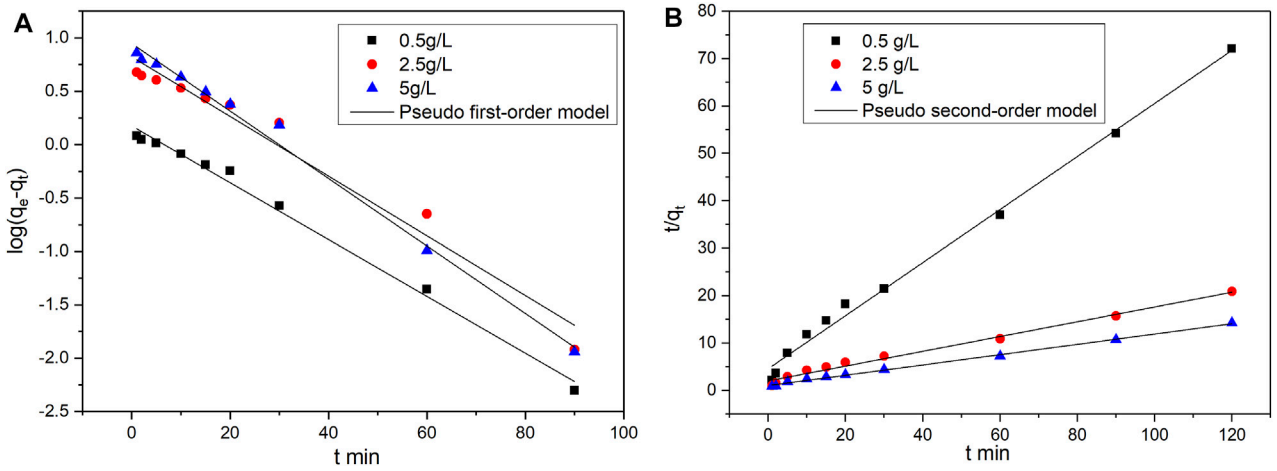

FIGURE 5 | Nonlinear fits of pseudo-first order and pseudo-second order kinetics models for vanadium ion adsorption by promoted catalyst. **(A)** Pseudo first-order model fitting; **(B)** Pseudo second-order model fitting.

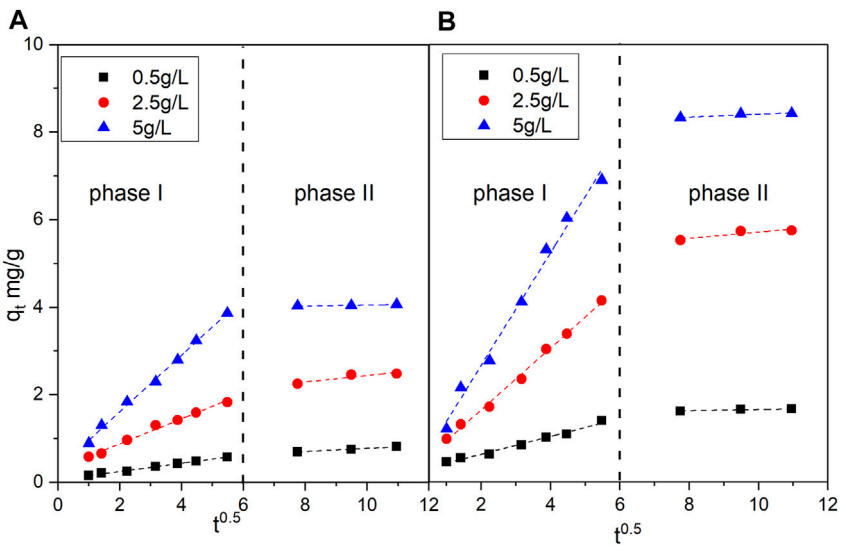

FIGURE 6 | Fitting curve of the intraparticle diffusion model for the adsorption of vanadyl ions by the **(A)** original catalyst and **(B)** promoted catalyst.

TABLE 3 | Kinetics parameters of the intraparticle diffusion model for the adsorption of vanadyl ions onto the original catalyst.

Intraparticle diffusion model	Parameters	Vanadyl ion concentration		
		0.5 g/L	2.5 g/L	5 g/L
Phase I	C_1(mg/g)	0.0619	0.308	0.3197
	$k_{i,1}$[mg/(g·min$^{0.5}$)]	0.0938	0.2869	0.647
	R^2	0.9937	0.9871	0.9959
Phase II	C_2(mg/g)	0.4149	1.7059	3.9479
	$k_{i,2}$[mg/(g·min$^{0.5}$)]	0.0362	0.0738	0.0106
	R^2	0.9908	0.7092	0.7928

TABLE 4 | Kinetics parameters of the intraparticle diffusion model for the adsorption of vanadyl ions onto the promoted catalyst.

Intraparticle diffusion model	Parameter	Vanadyl ion concentration		
		0.5 g/L	2.5 g/L	5 g/L
Phase I	C_1(mg/g)	0.2275	0.2385	0.1001
	$k_{i,1}$[mg/(g·min$^{0.5}$)]	0.2039	0.706	1.2845
	R^2	0.9822	0.9943	0.9877
Phase II	C_2(mg/g)	1.5163	4.995	8.0787
	$k_{i,2}$[mg/(g·min$^{0.5}$)]	0.014	0.0715	0.03247
	R^2	0.7367	0.6575	0.7354

TABLE 5 | The fitting parameters of Langmuir and Freundlich isotherm models for vanadium ion adsorption onto original catalyst.

Model	Parameters	293.15 K	308.15 K	323.15 K
Langmuir	q_m(mg/g)	3.716	4.734	5.614
	K_L(L/mg)	4.42×10^{-4}	3.48×10^{-4}	3.2×10^{-4}
	R^2	0.9111	0.9413	0.9683
Freundlich	K_F[(mg/g)/(mg/L)$^{1/n}$]	0.0115	0.0107	0.0116
	n(mg/L)	1.533	1.478	1.469
	R^2	0.969	0.964	0.978

TABLE 6 | The fitting parameters of Langmuir and Freundlich isotherm models for vanadium ion adsorption onto promoted catalyst.

Model	Parameters	293.15 K	308.15 K	323.15 K
Langmuir	q_m(mg/g)	6.82	9.966	14.443
	K_L(L/mg)	4.17×10^{-4}	3.48×10^{-4}	2.51×10^{-4}
	R^2	0.9779	0.9946	0.9871
Freundlich	K_F[(mg/g)/(mg/L)$^{1/n}$]	0.0313	0.0359	0.0265
	n(mg/L)	1.681	1.63	1.477
	R^2	0.9749	0.9753	0.9783

adsorption data fit the intraparticle diffusion model, the curve of q_t to $t^{0.5}$ is a straight line. If the regression line of q_t to $t^{0.5}$ is a single straight line and passes through the origin, this means that the adsorption process is mainly controlled by intraparticle diffusion. (Hu et al., 2014) By contrast, if multiple straight lines are observable, multiple processes such as intraparticle and interparticle diffusions have a strong effect on catalyst adsorption. (Li et al., 2013) The fitting results are shown in **Figure 6**.

As shown in **Figure 6**, the experimental data points for the adsorption of vanadyl ions onto the catalysts were mainly distributed on two straight lines. The straight line in phase I represents the interparticle diffusion process. The straight line in phase II represents the intraparticle diffusion process. The slope, intercept, and R^2 obtained through fitting are shown in **Tables 3**, **4**. The slopes of the two straight lines represent the interparticle diffusion process rate constant $k_{i,1}$ and the intraparticle diffusion process rate constant $k_{i,2}$, respectively. The fact that $k_{i,1}$ is considerably larger than $k_{i,2}$ indicated that the duration of interparticle diffusion was short. Moreover, the adsorption capacity achieved in interparticle diffusion exceeded that achieved in intraparticle diffusion.

Adsorption Equilibrium

The Langmuir and Freundlich adsorption isotherm equations (Tan et al., 2007; Ren et al., 2020), used to fit the adsorption data at various temperatures, are expressed as follows:

$$q_e = \frac{q_m K_L C_e}{1 + K_L C_e} \tag{6}$$

$$q_e = K_F C_e^{1/n} \tag{7}$$

where q_e is the adsorption capacity of the adsorbent at the adsorption equilibrium (mg/g); q_m is the theoretical saturated adsorption capacity (mg/g); C_e is the concentration of the adsorbate at the adsorption equilibrium (mg/L); K_L is the Langmuir adsorption equilibrium constant (L/mg); and K_F and n are Freundlich constants, which are related to the adsorption capacity and adsorption intensity, respectively.

Regarding the original catalyst (**Figure 7** and **Table 5**), the R^2 obtained under the Freundlich model was higher than that obtained under the Langmuir model. This indicated that the Freundlich model had a more satisfactory fitting result. Regarding the promoted catalyst (**Figure 8** and **Table 6**), the Langmuir model yielded a higher R^2 value, indicating that binding sites were uniformly distributed on the catalyst surface and that the adsorption of vanadyl ions onto the catalyst was dominated by monolayer adsorption.

SCR Performances

Figure 9 displays the effects of the original and promoted SCR catalysts on the DeNOx activity and SO_2/SO_3 conversion under the same vanadium adsorption capacity. The activity of the fresh SCR catalyst at 360°C was 40.6 m/h, and the SO_2/SO_3 conversion rate was 0.39%. According to the **Figure 9**, the DeNOx activity and SO_2/SO_3 conversion rate of the SCR catalyst after DMF modification were improved with the increase of vanadyl ion adsorption. Furthermore, the DeNOx activity of the promoted catalyst after reloading was significantly higher than that of the original catalyst, whereas the SO_2/SO_3 conversion rate was lower. After adsorbing 3.5 mg/g vanadium, the DeNOx activity of the reloaded original catalyst increased to 52.2 m/h (a 11.6 m/h increase), and the SO_2/SO_3 conversion rate increased to 1.22% (a 0.83% increase). After DMF modification, the DeNOx activity of the

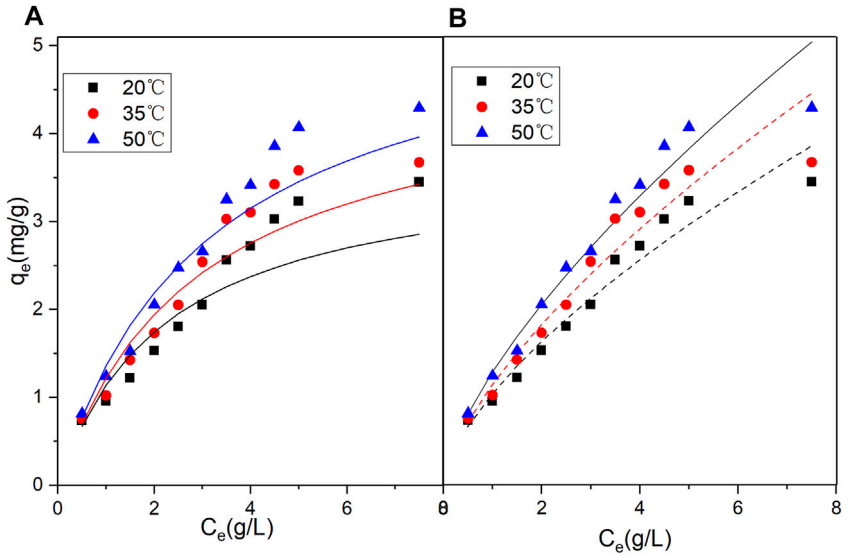

FIGURE 7 | Nonlinear fits of isotherm models for vanadium ion adsorption by original catalyst **(A)** Langmuir model **(B)** Freundlich model.

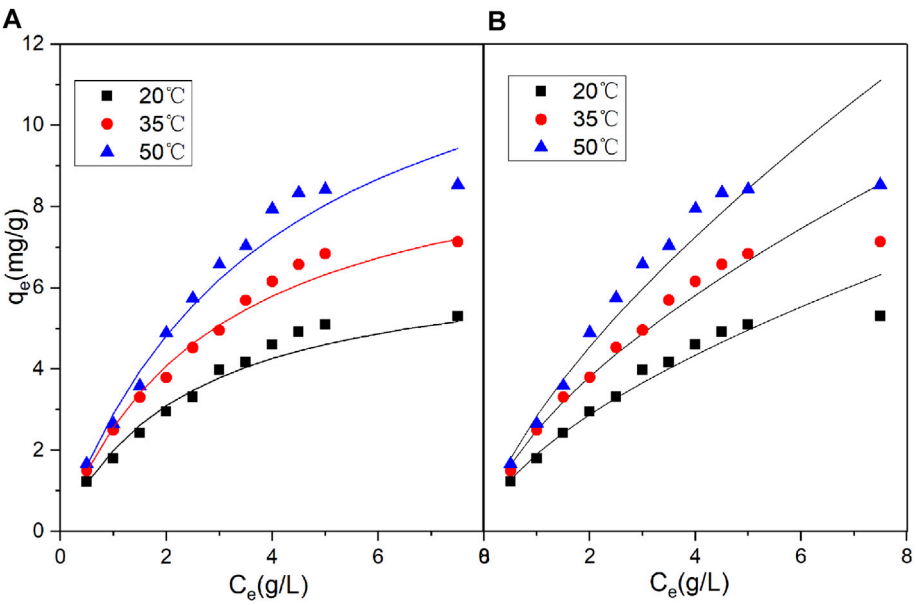

FIGURE 8 | Nonlinear fits of isotherm models for vanadium ion adsorption by promoted catalyst **(A)** Langmuir model **(B)** Freundlich model.

promoted catalyst increased to 60.1 m/h (a 19.5 m/h increase), 68.1% higher than that of the original catalyst. The SO_2/SO_3 conversion rate was 0.98% (a 0.59% increase), 28.9% lower than that of the original catalyst. This is because after DMF modification, a large number of functional groups remained on the catalyst surface. Vanadyl ions were first adsorbed onto the functional groups on the catalyst surface, greatly increasing the superficial vanadium content and limiting the increase in vanadium content within the catalyst. In the monolithic SCR catalyst, the DeNOx reaction of the catalyst occurred within 0.1 mm thin layer of the catalyst wall, whereas the SO_2/SO_3 conversion reaction occurred in the entire wall. Under the same loading, the promoted catalyst substantially increased the DeNOx activity and reduced the increase in the side reaction (SO_2/SO_3 conversion). In practical applications, the promoted catalyst can reduce the initial concentration of active components during the regeneration process and lower the loading of active components, which is conducive to the regeneration of SCR catalysts.

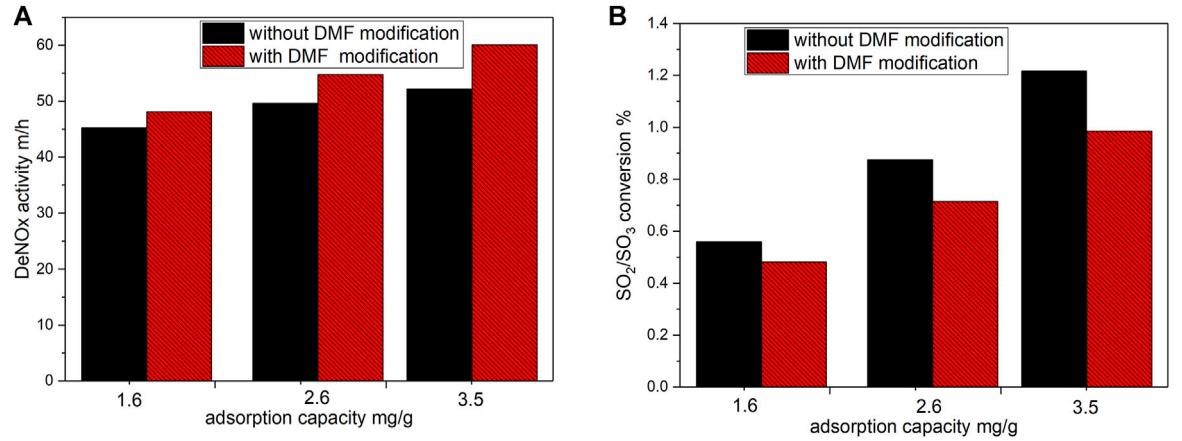

FIGURE 9 | Comparison of SCR performance and SO_2/SO_3 conversion between original and promoted catalysts. (Flow rate: 2.44 m^3/h, O_2:5%, NO, NH_3: 300 ppm, SO_2:500ppm, H_2O: 10%, Temperature: 360°C). **(A)** deNOx activity; **(B)** SO_2/SO_3 conversion

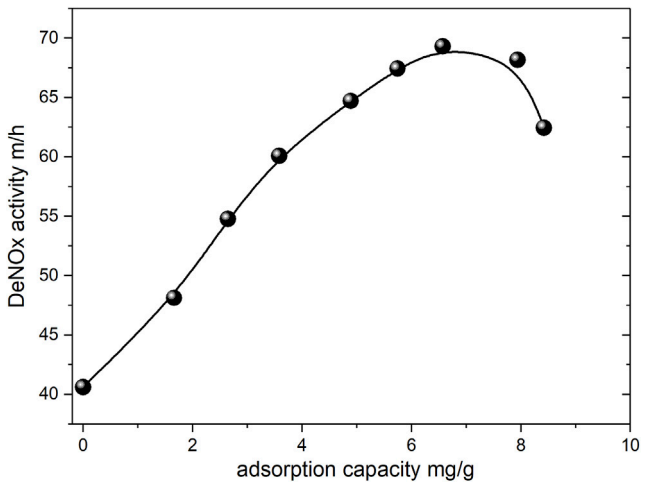

FIGURE 10 | Effect of V_2O_5 loading on DeNOx performance for promoted catalyst (Flow rate: 2.44 m^3/h, O_2:5%, NO, NH_3: 300 ppm, SO_2: 500ppm, H_2O: 10%, Temperature: 360°C).

Figure 10 presents the effect of various vanadium loadings on the DeNOx activity of the promoted catalyst. When the vanadium adsorption capacity increased from 0 to 6.5 mg/g, the DeNOx activity increased as the vanadium adsorption capacity increased, and the activity value increased from 40.6 to 69.3 m/h. However, when the vanadium adsorption capacity continued to increase, the DeNOx activity decreased. This phenomenon has two plausible explanations. The first is that in the adsorption process of the promoted catalyst, vanadyl ions were first adsorbed onto the functional groups on the catalyst surface when the concentration of vanadyl ions was low. Therefore, the DeNOx activity was greatly increased. However, as the concentration of vanadyl ions increased, in addition to the adsorption of vanadyl ions onto surface functional groups, vanadyl ions began entering the inner wall of the catalyst, resulting in the gradual adsorption of vanadyl ions in the catalyst pores. However, these vanadyl ions exerted only a limited effect on the increase in DeNOx activity (Kong et al., 2019). The second possibility is that after the catalysts were calcined, vanadyl ions were loaded onto the TiO_2 carrier in the form of V_2O_5 to form Ti–O–V bonds. At low adsorption capacity, V_2O_5 existed in the form of monomeric V_2O_5 on the catalyst surface (Busca et al., 1998; Bulushev et al., 2001), and with the increase in the vanadium adsorption capacity, V_2O_5 gradually formed multimer and V_2O_5 crystals (Oyama et al., 2002; He et al., 2018). The V_2O_5 crystals were not conducive to the SCR reaction due to weak V–O–Ti bonds. Therefore, as the vanadium adsorption capacity continuously increased, the DeNOx activity decreased.

CONCLUSION

The conclusion of this study are summarized as follows:

First, DMF was employed to improve the performance for the adsorption of vanadyl ions. When the concentration of the DMF was increased, the vanadyl ion adsorption capacity of the promoted catalyst first increased and then decreased. DMF modification was effective in improving the adsorption capacity of the promoted catalyst.

Second, the adsorption kinetics demonstrated that the pseudo-second-order kinetics model better describes the process by which vanadyl ions adsorb onto different catalysts. Moreover, the adsorption rate was both controlled by intraparticle and interparticle diffusion. In addition, the adsorption equilibrium results indicated that the Freundlich model was a more favorable fit for the vanadyl ion adsorption to the original catalyst while Langmuir model was a closer fit for the promoted catalyst.

Third, the DeNOx activity results revealed that after DMF modification, limited increase in vanadium content within the interior of catalyst was conducive to enhancing the DeNOx activity and reducing the increase in the SO_2/SO_3 conversion. The initial concentration of active components and the loading of active components in the actual activation process were reduced, thereby promoting the regeneration of SCR catalysts.

DATA AVAILABILITY STATEMENT

The raw data supporting the conclusion of this article will be made available by the authors, without undue reservation.

AUTHOR CONTRIBUTIONS

Conceptualization, CZ and SL; methodology, CZ; investigation, HS, JG, and WW; writing—original draft preparation, HS and YZ; writing—review and editing, SL; supervision, XG

FUNDING

This work was supported by the National Key Research and Development Program of China under the Grant No. 2021YFB2601605, the National Natural Science Foundation of China (51836006), and the Fund for Longquan Innovation Center of Zhejiang University(ZDLQ 2020003).

REFERENCES

Addy, M., Losey, B., Mohseni, R., Zlotnikov, E., and Vasiliev, A. (2012). Adsorption of Heavy Metal Ions on Mesoporous Silica-Modified Montmorillonite Containing a Grafted Chelate Ligand. *Appl. Clay Sci.* 59-60, 115–120. doi:10.1016/j.clay.2012.02.012

Bulushev, D. A., Rainone, F., Kiwi-Minsker, L., and Renken, A. (2001). Influence of Potassium Doping on the Formation of Vanadia Species in V/Ti Oxide Catalysts. *Langmuir* 17, 5276–5282. doi:10.1021/la010077g

Busca, G., Lietti, L., Ramis, G., and Berti, F. (1998). Chemical and Mechanistic Aspects of the Selective Catalytic Reduction of NO by Ammonia over Oxide Catalysts: A Review. *Appl. Catal. B: Environ.* 18, 1–36. doi:10.1016/s0926-3373(98)00040-x

Dunn, J. P., Koppula, P. R., G. Stenger, H., and Wachs, I. E. (1998). Oxidation of Sulfur Dioxide to Sulfur Trioxide over Supported Vanadia Catalysts. *Appl. Catal. B: Environ.* 19, 103–117. doi:10.1016/s0926-3373(98)00060-5

Forzatti, P., Nova, I., and Beretta, A. (2000). Catalytic Properties in deNOx and SO2-SO3 Reactions. *Catal. Today* 56, 431–441. doi:10.1016/s0920-5861(99)00302-8

Forzatti, P. (2001). Present Status and Perspectives in De-NOx SCR Catalysis. *Appl. Catal. A: Gen.* 222, 221–236. doi:10.1016/s0926-860x(01)00832-8

Gao, Q., Zhu, H., Luo, W.-J., Wang, S., and Zhou, C.-G. (2014). Preparation, Characterization, and Adsorption Evaluation of Chitosan-Functionalized Mesoporous Composites. *Microporous Mesoporous Mater.* 193, 15–26. doi:10.1016/j.micromeso.2014.02.025

He, G., Lian, Z., Yu, Y., Yang, Y., Liu, K., Shi, X., et al. (2018). Polymeric Vanadyl Species Determine the Low-Temperature Activity of V-Based Catalysts for the SCR of NO X with NH3. *Sci. Adv.* 4, eaau4637. doi:10.1126/sciadv.aau4637

Hu, X.-j., Liu, Y.-g., Zeng, G.-m., Wang, H., Hu, X., Chen, A.-w., et al. (2014). Effect of Aniline on Cadmium Adsorption by Sulfanilic Acid-Grafted Magnetic Graphene Oxide Sheets. *J. Colloid Interf. Sci.* 426, 213–220. doi:10.1016/j.jcis.2014.04.016

Jiang, L., Liu, Q., Ran, G., Kong, M., Ren, S., Yang, J., et al. (2019). V2O5-modified Mn-Ce/AC Catalyst with High SO2 Tolerance for Low-Temperature NH3-SCR of NO. *Chem. Eng. J.* 370, 810–821. doi:10.1016/j.cej.2019.03.225

Khodayari, R., and Ingemar Odenbrand, C. U. (2001). Regeneration of Commercial SCR Catalysts by Washing and Sulphation: Effect of Sulphate Groups on the Activity. *Appl. Catal. B: Environ.* 33, 277–291. doi:10.1016/s0926-3373(01)00193-x

Khodayari, R., and Odenbrand, C. U. I. (2001). Regeneration of Commercial TiO2-V2o5-WO3 SCR Catalysts Used in Bio Fuel Plants. *Appl. Catal. B: Environ.* 30, 87–99. doi:10.1016/s0926-3373(00)00227-7

Kong, M., Liu, Q., Jiang, L., Tong, W., Yang, J., Ren, S., et al. (2019). K+ Deactivation of V2O5-WO3/TiO2 Catalyst during Selective Catalytic Reduction of NO with NH3: Effect of Vanadium Content. *Chem. Eng. J.* 370, 518–526. doi:10.1016/j.cej.2019.03.156

Kong, M., Liu, Q., Wang, X., Ren, S., Yang, J., Zhao, D., et al. (2015). Performance Impact and Poisoning Mechanism of Arsenic over Commercial V2O5-WO3/TiO2 SCR Catalyst. *Catal. Commun.* 72, 121–126. doi:10.1016/j.catcom.2015.09.029

Kong, M., Liu, Q., Zhu, B., Yang, J., Li, L., Zhou, Q., et al. (2015). Synergy of KCl and Hgel on Selective Catalytic Reduction of NO with NH3 over V2O5-WO3/TiO2 Catalysts. *Chem. Eng. J.* 264, 815–823. doi:10.1016/j.cej.2014.12.038

Li, T.-t., Liu, Y.-g., Peng, Q.-q., Hu, X.-j., Liao, T., Wang, H., et al. (2013). Removal of Lead(II) from Aqueous Solution with Ethylenediamine-Modified Yeast Biomass Coated with Magnetic Chitosan Microparticles: Kinetic and Equilibrium Modeling. *Chem. Eng. J.* 214, 189–197. doi:10.1016/j.cej.2012.10.055

Li, X., Li, X., Chen, J., Li, J., and Hao, J. (2016). An Efficient Novel Regeneration Method for Ca-Poisoning V2O5-WO3/TiO2 Catalyst. *Catal. Commun.* 87, 45–48. doi:10.1016/j.catcom.2016.06.017

Luo, W.-J., Gao, Q., Wu, X.-L., and Zhou, C.-G. (2014). Removal of Cationic Dye (Methylene Blue) from Aqueous Solution by Humic Acid-Modified Expanded Perlite: Experiment and Theory. *Separat. Sci. Technol.* 49, 2400–2411. doi:10.1080/01496395.2014.920395

Orsenigo, C., Beretta, A., Forzatti, P., Svachula, J., Tronconi, E., Bregani, F., et al. (1996). Theoretical and Experimental Study of the Interaction between NOx Reduction and SO2 Oxidation over DeNOx-SCR Catalysts. *Catal. Today* 27, 15–21. doi:10.1016/0920-5861(95)00168-9

Oyama, S. T., Went, G. T., Lewis, K. B., Bell, A. T., and Somorjai, G. A. (2002). Oxygen Chemisorption and Laser Raman Spectroscopy of Unsupported and Silica-Supported Vanadium Oxide Catalysts. *J. Phys. Chem.* 93, 6786–6790. doi:10.1021/j100355a041

Peng, Y., Li, J., Si, W., Luo, J., Wang, Y., Fu, J., et al. (2015). Deactivation and Regeneration of a Commercial SCR Catalyst: Comparison with Alkali Metals and Arsenic. *Appl. Catal. B: Environ.* 168-169, 195–202. doi:10.1016/j.apcatb.2014.12.005

Ren, X. Y., Liu, S. J., Qu, R. Y., Xiao, L. F., Hu, P., Song, H., et al. (2020). Synthesis and Characterization of Single-phase Submicron Zeolite Y from Coal Fly Ash and its Potential Application for Acetone Adsorption. *Microporous Mesoporous Mater.* 295, 13. doi:10.1016/j.micromeso.2019.109940

Song, H., Liu, S., Zhang, M., Wu, W., Qu, R., Zheng, C., et al. (2018). A Comparative Study of the NH 3-SCR Reactions over an Original and Sb-Modified V 2 O 5–WO 3/TiO 2 Catalyst at Low Temperatures. *Energies* 11, 1–13. doi:10.3390/en11123339

Song, H., Zhang, M., Yu, J., Wu, W., Qu, R., Zheng, C., et al. (2018). The Effect of Cr Addition on Hg0 Oxidation and NO Reduction over V2O5/TiO2 Catalyst. *Aerosol Air Qual. Res.* 18, 803–810. doi:10.4209/aaqr.2017.10.0411

Tan, I. A. W., Hameed, B. H., and Ahmad, A. L. (2007). Equilibrium and Kinetic Studies on Basic Dye Adsorption by Oil palm Fibre Activated Carbon. *Chem. Eng. J.* 127, 111–119. doi:10.1016/j.cej.2006.09.010

Tanno, K., Makino, H., Kurose, R., Komori, S., Shimada, H., and Hwang, S.-M. (2010). Effect of Turbulent-Laminar Flow Transition on Degradation of De-NOx Catalyst. *Fuel* 89, 855–858. doi:10.1016/j.fuel.2009.03.028

Tronconi, E., Beretta, A., Elmi, A. S., Forzatti, P., Malloggi, S., and Baldacci, A. (1994). A Complete Model of Scr Monolith Reactors for the Analysis of Interacting Nox Reduction and So2 Oxidation Reactions. *Chem. Eng. Sci.* 49, 4277–4287. doi:10.1016/s0009-2509(05)80021-1

Tronconi, E., Cavanna, A., Orsenigo, C., and Forzatti, P. (1999). Transient Kinetics of SO2 Oxidation over SCR-DeNOx Monolith Catalysts. *Ind. Eng. Chem. Res.* 38, 2593–2598. doi:10.1021/ie980673e

Wang, S., Zhai, Y.-Y., Gao, Q., Luo, W.-J., Xia, H., and Zhou, C.-G. (2013). Highly Efficient Removal of Acid Red 18 from Aqueous Solution by Magnetically Retrievable Chitosan/Carbon Nanotube: Batch Study, Isotherms, Kinetics, and Thermodynamics. *J. Chem. Eng. Data* 59, 39–51. doi:10.1021/je400700c

Xi, Y., Su, C., Ottinger, N. A., and Gerald Liu, Z. (2020). Effects of Hydrothermal Aging on the Sulfur Poisoning of a Cu-SSZ-13 SCR Catalyst. *Appl. Catal. B: Environ.* 284, 119749. doi:10.1016/j.apcatb.2020.119749

Xiong, S., Chen, J., Huang, N., Yan, T., Peng, Y., and Li, J. (2020). The Poisoning Mechanism of Gaseous HCl on Low-Temperature SCR Catalysts: MnO –CeO2 as an Example. *Appl. Catal. B: Environ.* 267, 118668. doi:10.1016/j.apcatb.2020.118668

Yao, X., Kang, K., Cao, J., Chen, L., Luo, W., Zhao, W., et al. (2020). Enhancing the Denitration Performance and Anti-K Poisoning Ability of CeO2-TiO2/P25 Catalyst by H2SO4 Pretreatment: Structure-Activity Relationship and Mechanism Study. *Appl. Catal. B: Environ.* 269, 118808. doi:10.1016/j.apcatb.2020.118808

Yu, Y., He, C., Chen, J., Yin, L., Qiu, T., and Meng, X. (2013). Regeneration of Deactivated Commercial SCR Catalyst by Alkali Washing. *Catal. Commun.* 39, 78–81. doi:10.1016/j.catcom.2013.05.010

Yuan, P., Liu, D., Tan, D.-Y., Liu, K.-K., Yu, H.-G., Zhong, Y.-H., et al. (2013). Surface Silylation of Mesoporous/macroporous Diatomite (Diatomaceous Earth) and its Function in Cu(II) Adsorption: The Effects of Heating Pretreatment. *Microporous Mesoporous Mater.* 170, 9–19. doi:10.1016/j.micromeso.2012.11.030

Zhang, Y., Zheng, C., Liu, S., Wu, W., Yang, Y., Zhao, H., et al. (2020). Investigation of Arsenic Poisoned Selective Catalytic Reduction Catalyst Performance and Lifetime in Coal-Fired Power Plants. *Energy Fuels* 34, 12833–12840. doi:10.1021/acs.energyfuels.0c02227

Conflict of Interest: The authors declare that the research was conducted in the absence of any commercial or financial relationships that could be construed as a potential conflict of interest.

Publisher's Note: All claims expressed in this article are solely those of the authors and do not necessarily represent those of their affiliated organizations, or those of the publisher, the editors and the reviewers. Any product that may be evaluated in this article, or claim that may be made by its manufacturer, is not guaranteed or endorsed by the publisher.

Copyright © 2022 Song, Guo, Liu, Zhang, Wu, Zheng and Gao. This is an open-access article distributed under the terms of the Creative Commons Attribution License (CC BY). The use, distribution or reproduction in other forums is permitted, provided the original author(s) and the copyright owner(s) are credited and that the original publication in this journal is cited, in accordance with accepted academic practice. No use, distribution or reproduction is permitted which does not comply with these terms.